Organic Electronics 10 (2009) 352–356

Contents lists available at ScienceDirect

Organic Electronics

journal homepage: www.elsevier.com/locate/orgel

Letter

Highly efficient photovoltaic diode based organic ultraviolet photodetector and the strong electroluminescence resulting from pure exciplex emission

Guang Zhang [a], Wenlian Li [a,*], Bei Chu [a,*], Zisheng Su [a], Dongfang Yang [a], Fei Yan [a], Yiren Chen [a], Dongyu Zhang [a], Liangliang Han [a], Junbo Wang [a], Huihui Liu [a], Guangbo Che [a], Zhiqiang Zhang [b], Zhizhi Hu [b]

[a] Key Laboratory of Excited State Processes, Changchun Institute of Optics, Fine Mechanics and Physics, Chinese Academy of Sciences, 16-Dong NanHu Road, Changchun, Jilin 130033, PR China
[b] Organic Photoelectronic Materials and Technology Development Center, Liaoning University of Science and Technology, Anshan 114000, PR China

ARTICLE INFO

Article history:
Received 9 July 2008
Received in revised form 28 October 2008
Accepted 3 November 2008
Available online 20 November 2008

PACS:
72.40.+w

Keywords:
Ultraviolet photodetector
Exciplex
Photovoltaic

ABSTRACT

We demonstrate organic photovoltaic (PV) and ultraviolet (UV) photodetector devices using 1,3,5-tris(3-methylphenyl-phenylamino)-triphenyamine and 1,3,5-tris(N-phenyl-benzimidazol-2-yl)-benzene to function as the donor (D) and the acceptor (A), respectively. Two types of structural devices, a planar heterojunction of layer-by-layer and a bulk heterojunction with a D/A blend layer are fabricated, respectively. Under UV-365 irradiation, the PHJ device offers a power conversion efficiency of ~10%, while the BHJ device behaves with a responsivity of 135 mA/W at −4 V bias. The BHJ device can also obtain a high exciplex electroluminescence (EL). The dependencies of PV and EL performances on exciplex formation were also discussed.

Ultraviolet (UV) sensitive photovoltaic (PV) diodes can be used for environment monitoring, combustion flames, UV curing monitors, developing areas, and so on [1–7]. Moreover, the devices, especially the visible–blind (VB) device, also has potential applications in solar astronomy, missile plume detection, space-to-space transmission, and sterilization monitors. The wide-band-gap inorganic photodetectors based III-nitrides [2], SiC [3] and II–VI materials [4] are constructed on expensive substrates such as sapphire [5] or SiC [3], and the associated fabrication techniques are troublesome and costly. Differing from inorganic systems, organic UV photodetectors have undergone rapid development in recent years, which can be ascribed to simpler fabrication processes, lighter weight and lower costs [6,7]. However, organic UV photodetectors still exhibit lower responsivity, such as a peak responsivity of 30 mA/W [6]. Organic PV performances rely intensively on electrical properties including energy levels and the carrier mobility of the donor (D) and acceptor (A) materials and the diode structure. For this reason, we will select a new material system in which the D material has a low ionization potential (IP) and the A material presents a higher electron affinity (EA) and electron-mobility. 1,3,5-*tris*(3-methylphenyl-phenylamino)-triphenyamine (m-MTDATA) is a well- known effective D materiel due to its lower IP (5.1 eV) and high hole mobility of 3×10^{-5} cm^2/Vs [8]. It has also been studied on various exciplex-type devices [9–11]. However, the efficiency of m-MTDATA based PV devices shows lower performance which may be due to the unmatched energy alignment between m-MTDATA and

* Corresponding authors.
E-mail addresses: wllioel@yahoo.com.cn (W. Li), beichu@163.com (B. Chu).

1566-1199/$ - see front matter © 2008 Elsevier B.V. All rights reserved.
doi:10.1016/j.orgel.2008.11.006

bathocuproine (BCP) [11]. Compared with BCP as an acceptor, 1,3,5-*tris*(*N*-phenyl-benzimidazol-2-yl) benzene (TPBi) presents a higher electron mobility (EM) over BCP and *tris*-(8-hydroxy-quinoline) aluminum (Alq_3) [12]. Its electron mobility increases three times than that of BCP when the applied electrical field increased only two times, which lead to a decisive PV performance. TPBi is generally used as the exciton blocking and electronic transporting material to substitute BCP/Alq_3 layers in the field of OLED fabrications. In this Letter, a new PV diode was constructed where m-MTDATA and TPBi serve as D and A, respectively, and BCP was also employed as the exciton blocking layer (EBL).

All devices were fabricated on cleaned glass substrates pre-coated with conducting indium–tin–oxide (ITO) anode with a sheet resistance of 25 Ω/sq, and the substrates were treated by UV ozone in a chamber for 15 min after solvent cleaning. The organic films were thermally evaporated in high vacuum ($<10^{-6}$ Torr) using previously calibrated quartz crystal monitors to determine the deposition rate and the film thickness. The organic layers were deposited at a rate of 2 Å/s. The evaporating rate of LiF and Al cathode were controlled to be 0.5 Å/s and 10 Å/s with the thickness of 10 Å and 2000 Å, respectively. A 365 nm UV light with a power of 0.426 mW/cm^2 was employed to illuminate both types of diodes at zero bias and various reverse biases.

Fig. 1 shows the chemical structures of the used materials and the schematic energy level diagram of the PHJ device. The function of three layers has been expatiated in the preamble. About 10 Å LiF was used as the complex cathode with Al to further increase the performance [13,14]. To compare the performance of the diodes, two types of devices were constructed. One is device-A with a structure of ITO/m-MTDATA(350 Å)/TPBi(500 Å)/BCP(120 Å)/LiF(10 Å)/Al. The other is device-B with a structure of ITO/m-MTDATA(300 Å)/m-MTDATA:TPBi (1:1, 100 Å)/TPBi(450 Å)/BCP(120 Å)/LiF(10 Å)/Al, which were called the planar heterojunction (PHJ) and bulk-heterojunction (BHJ) devices hereafter, respectively.

Fig. 2a shows *I–V* characteristics of the PHJ and BHJ devices. According to the figure, the open-circuit voltage (V_{OC}), short-circuit current density (J_{SC}), and fill factor (*FF*) for PHJ and BHJ devices were 2.26 and 2.22 V, 46.1 and 46.7 μA/cm^2, 37.5% and 31.3%, yielding a power conversion efficiency (η_p) of 9.15% and 7.63%, respectively. Compared with previous reports [15], the η_p of 9.15% is highest found until now. The above data depicts that η_p is higher for PHJ than for BHJ structure devices. It is

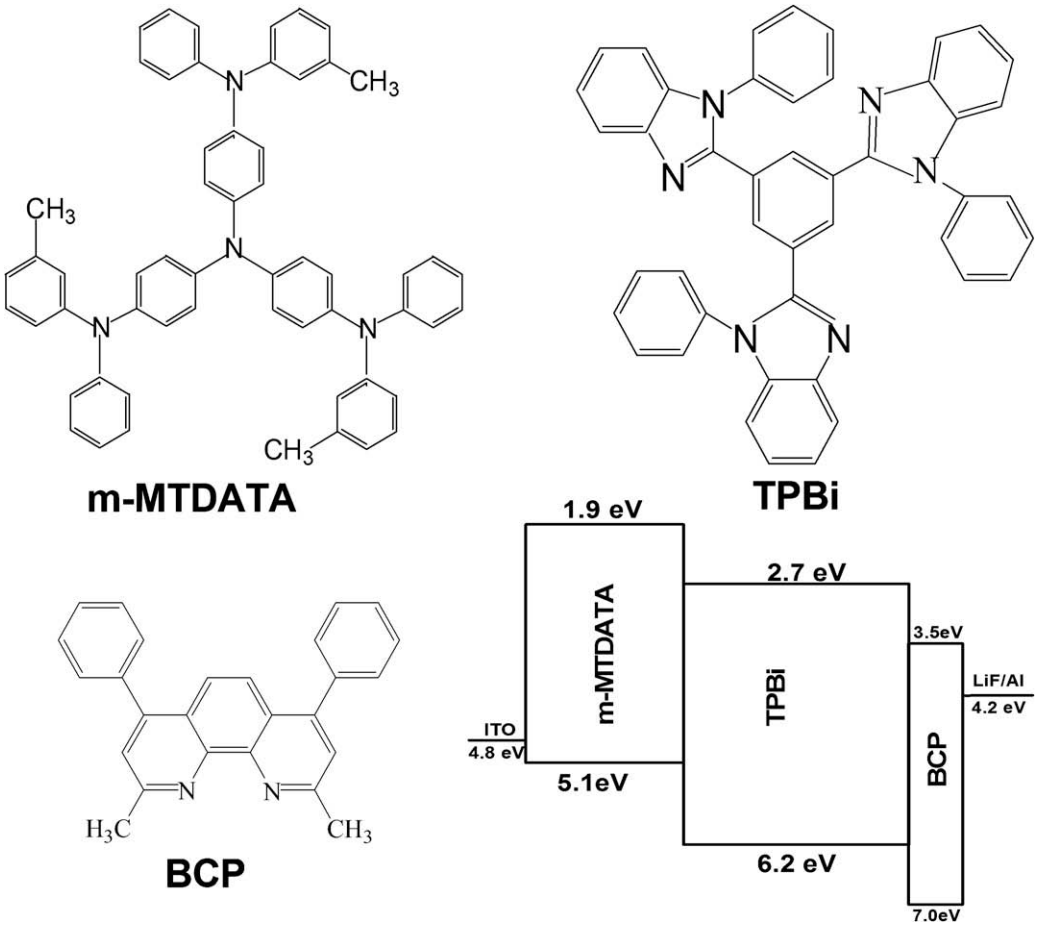

Fig. 1. Materials and schematic energy-level diagram of the PHJ device used in this work with the highest occupied molecular orbital (HOMO) level and the lowest unoccupied molecular orbital (LUMO) level which were cited from literatures (see Ref. [20,21]).

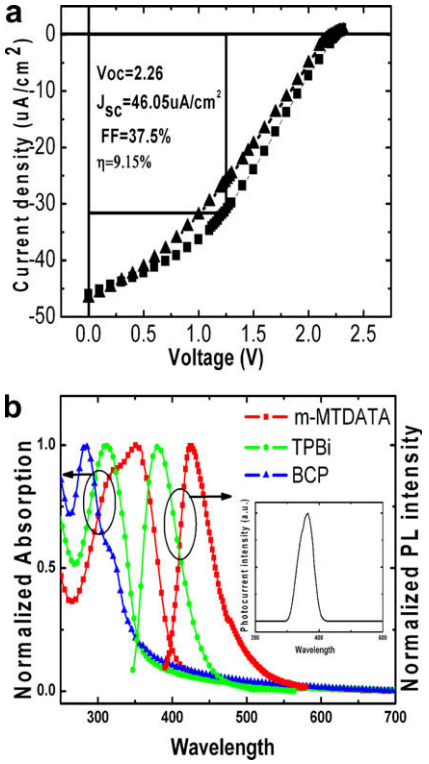

Fig. 2. (a) *I–V* characteristics of the PHJ device (filled block) and BHJ device (filled triangle) under irradiation at 365 nm at an incident light density of 0.426 mW/cm^2. (b) Normalized absorption and PL spectra of neat m-MTDATA, TPBi and BCP neat films on quartz substrates. The insert shows the same photocurrent spectral response of PHJ and BHJ-devices.

interesting that this result is very different from the previous relationship in which the blend-device (BHJ) generally provides a higher PV property than that of a bilayer (PHJ) device reported in Yang's work [16]. The discrepancy in the phenomena of PV efficiency can be understood as follows. First of all, BHJ devices can provide a large interface area where photoinduced charge transfer by excitons into separated electrons and holes can efficiently occur. In this case, excitons are always generated within a diffusion length (~3–10 nm) of a donor–acceptor interface, potentially leading to higher cell efficiency than a planar heterojunction. Secondly, m-MTDATA is an amorphous film. It possesses a denser film structure and finer surface morphology than CuPc microcrystalline [17]. Because the charge mobility is higher in crystalline than in amorphous materials, the existence of crystalline structures is important for ensuring a low cell series resistance [16]. Thirdly, the mean distance between neighboring molecules of the same species in the mixed layer is larger than that in their respective homogeneous layers. The hopping mobilities are expected to decrease upon intermixing on the molecular scale. Both the second and third reasons lead to a larger internal series resistance in our BHJ device, which result in a lower *FF*, i.e., the *FF* is lower for the BHJ-device (0.313) than for the PHJ-device (0.375), consequently a lower η_p for the BHJ-device. In other words, the introduction of the blend layer produces a pair of contradictory processes and results in a trade-off in which the highest η_p can be obtained. However, when the thickness of blend layer decreases from 20 to 2 nm, the η_p increases linearly and the maximum photocurrent is highest only at 10 nm. This suggested that the method of mixing D:A could be unfit for our system, and the causes will be illuminated at the latter of part of this paper.

Fig. 2b shows the normalized absorption and photoluminescence (PL) spectra of neat m-MTDATA, TPBi and BCP neat films on quartz substrates as well as the photocurrent spectral response of the PHJ-device. In the insert of Fig. 2b, it shows that both types of devices offer the same photocurrent spectral responses which mainly correspond with the absorption of m-MTDATA film. It proved that most of the excitons were generated in the m-MTDATA layer. An absorption peak of TPBi is located at 315 nm, at which the photons can be completely absorbed by ITO glass, leading to a smaller contribution of spectral response in TPBi layer. The spectral response is located at the band from 300 to 400 nm, which is just at the VB UV spectral position. We also found that these two types of diodes have a higher photoelectric detector effect under the irradiation of 365 nm UV light.

Fig. 3a depicts the dark-corrected photocurrent response as a function of the different reverse bias for the two types of devices. It is clearly shown that generation rate of the free carrier is prominently enhanced with the increase of the reverse bias voltage and gradually reach a

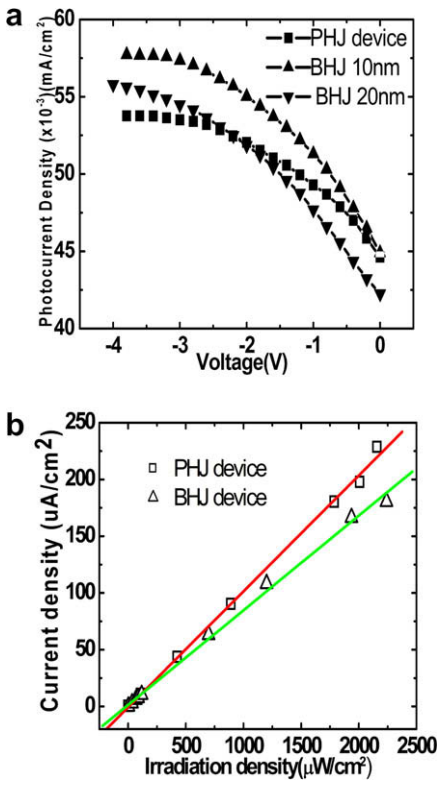

Fig. 3. (a) Dark-corrected photocurrent response as a function of different reverse biases for the different structure detector devices. (b) Dependence of photocurrent response on the 365 UV irradiation intensity at zero bias.

saturation value. The BHJ device has a higher photocurrent and saturation photocurrent density than the PHJ one, which is due to a higher amount of intermolecular contact between the D/A, which proves that the generation and disassociation ratio of the exction in the BHJ device is easier than that of the PHJ. The difference between the photocurrents gradually increases with the increase of the reverse bias which indicates that the external electric field gradually plays a leading role over the built-in electric field. But the case is different when the thickness of the mixed layer is increased to 20 nm. That is, at lower reverse bias, the responsivity is higher for the PHJ device than for the BHJ one because the built-in field plays a dominating role in exciton dissociation. But as the reverse bias increases, the external electrical field plays a dominant role in exciton dissociation for the BHJ device, because the external electrical filed could overcome the disadvantageous influence of the higher resistance at the blend layer while taking advantage of the much higher photogenerated exciton ratio, thus the photocurrent will be higher than that of the PHJ one but lower than the optimized BHJ device with a 10 nm blend layer (see Fig. 3a).

The dependence of the photocurrent response on the incident UV light intensity under zero bias was shown in Fig. 3b. From the slope of the fitted line, the responsivities of 100 and 85 mA/W for the PHJ and BHJ detectors were attained, respectively, which is three times higher than that reported by Ray's [6] and can be compared with that of GaN (~100 mA/W) and of SiC (130 mA/W) based on inorganic UV detectors [2,3]. When the reverse bias rises to 4 V, the responsivity of the BHJ structure based the detector can up to 135 mA/W, and the photodetector presents a constant at broad irradiation density range with only a sharp spectral response as shown in the insert of Fig. 2b.

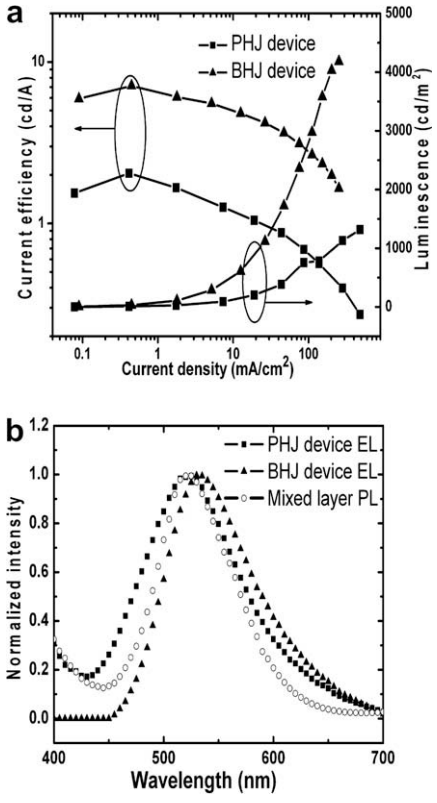

Fig. 4. (a) Plot of current efficiency and luminance as a function of current density for PHJ device and BHJ device. (b) The EL spectra of PHJ and BHJ devices and the PL spectrum of BHJ device.

Fig. 4a provides the current efficiency and luminance as a function of current density for the two devices. Fig. 4b indicates the EL and PL spectra of the PHJ and BHJ-structure devices. Both the PHJ and BHJ devices show a bright green emission peak at 520 nm, which are completely different from the emission spectrum of m-MTDATA and TPBi monomers, proving it is caused by exciplex [10]. Exciplex is formed at the intermolecular interface between the excited state of m-MTDATA and the ground state of TPBi molecules [18]. We note that the emission of the BHJ and PHJ devices exhibit the maximum current efficiencies of 7.14 and 2.05 cd/A, and the peak luminance of 4182 and 1319 cd/m^2, at 8.2 V and 7.5 V biases, respectively. That means these two types of devices have an EL effect and a PV effect, which were connected by exciplex and will be explained as below. There is a weak emission at blue waveband even extending to UV area in PHJ EL device and it increases with applied voltage. It is because the exciplex formation takes place only at the interface between m-MTDATA and TPBi. The increasing in the applied voltage leads to an increase in the number of injected holes and electrons, which recombine not only at the interface but also in the bulk of the TPBi layer, which can be proved from the PL spectrum of TPBi.

It is well known that the energy level offset of D and A at heterojunctions interface plays a very important role in the operation of the PV diode because exciton dissociation occurs at the D/A interface, while exciplex can be formed in the same place in some system. Based on our previous experiments [9,10,19], the formation of exciplex would be easier in the BHJ than for the PHJ structure device as there is a higher number of D/A molecular interactions. That is, the intensity of exciplex EL is higher for the BHJ device. Compared with the EL result, there is a contrary dependence on the PV performance in our system. That is, the PHJ device offers higher PV properties and better EL performance but its PL of exciplex is almost indetectable (data not shown), which is due to less contact and interaction among D/A molecules, while the BHJ device offers lower PV properties and better EL performance and its intensive PL of exciplex which is due to much more contact and interaction between D/A molecules (see Fig. 4b).

We deduced that there would be a competitive process between exciplex formation and photo-generated free charge carriers. Thus we supposed that they have a common precursor, which is most likely a similar non-emissive geminate pair. The PL of exciplex competes with the PV effect, which leads to a lower PV effect. The dynamic physical process may be like this: When the PV device was irradiated by a photon of a suitable energy, photo-generated excitons diffuse to the interface of the heterojunction and converse into non-emissive geminate pairs, and they are the generated common precursor. They will transform either into exciplex and emit photons or free charge carriers that drive the external circuit load. However, the

dynamic factors that decide what the common precursor will change into are still confusing.

In conclusion, we have fabricated a high efficiency PHJ-PV device with the η_p of 9–10%. This diode could be used as a photodetector for its sharp response in VB-UV and a responsivity of 100 mA/W at zero bias. A maximum responsivity of 135 mA/W was achieved in the BHJ device with a 10 nm blend layer with 1:1 D:A at a −4 bias, while this device has peak current efficiency and maximum luminance of 7.14 cd/A and 4182 cd/m^2 under electrical excitation. A new dependence of the PV and EL performances on the exciplex formation was discovered in our small molecular system, which will inspire us to design more efficient organic electronic diode devices.

Acknowledgement

This work was supported by the National Natural Science Foundation of China under Grant No. 60877027.

References

[1] M. Razeghi, A. Rogalski, J. Appl. Phys. 79 (1996) 7433.
[2] B. Butun, T. Tut, E. Ulker, T. Yelboga, E. Ozbay, Appl. Phys. Lett. 92 (2008) 033507.
[3] X. Chen, H. Zhu, J. Cai, Z. Wu, J. Appl. Phys. 102 (2007) 024505.
[4] A. Ohtomo, M. Kawasaki, Y. Sakurai, Y. Yoshida, H. Koinuma, P. Yu, Z.K. Tang, G.K.L. Wong, Y. Segawa, Mater. Sci. Eng. B 54 (1998) 24.
[5] Y.D. Jhou, S.J. Chang, Y.K. Su, Y.Y. Lee, C.H. Liu, H.C. Lee, Appl. Phys. Lett. 91 (2007) 103506.
[6] D. Ray, K.L. Narasimhan, Appl. Phys. Lett. 91 (2007) 093516.
[7] T.P.I. Saragi, M. Fetten, J. Salbeck, Appl. Phys. Lett. 90 (2007) 253506.
[8] C. Giebeler, H. Antoniadis, D.D.C. Bradley, Y. Shirota, Appl. Phys. Lett. 72 (1998) 2448.
[9] W.M. Su, W.L. Li, Q. Xin, Z.S. Su, B. Chu, D.F. Bi, H. He, J.H. Niu, Appl. Phys. Lett. 91 (2007) 043508.
[10] M. Li, W. Li, L. Chen, Z. Kong, B. Chu, B. Li, Z. Hu, Z. Zhang, Appl. Phys. Lett. 88 (2006) 091108.
[11] L.L. Chen, W.L. Li, M.T. Li, B. Chu, J. Lumin. 122–123 (2007) 667.
[12] Y.Q. Li, M.K. Fung, Z.Y. Xie, S.T. Lee, L.S. Hung, J. Shi, Adv. Mater. 14 (2002) 1317.
[13] C.J. Brabec, S.E. Shaheen, C. Winder, N.S. Sariciftci, P. Denk, Appl. Phys. Lett. 80 (2002) 1288.
[14] A.K. Pandey, K.N.N. Unni, J.-M. Nunzi, Thin Solid Films 511–512 (2006) 529.
[15] J.Y. Kim, K. Lee, N.E. Coates, D. Moses, T.-Q. Nguyen, M. Dante, A.J. Heeger, Science 317 (2007) 222.
[16] F. Yang, M. Shtein, S.R. Forrest, Nat. Mater. 4 (2005) 37.
[17] S.-F. Chen, C.-W. Wang, Appl. Phys. Lett. 85 (2004) 765.
[18] H.O.Y.S. Tetsuya Noda, Adv. Mater. 11 (1999) 283.
[19] D. Wang, W. Li, B. Chu, Z. Su, D. Bi, D. Zhang, J. Zhu, F. Yan, Y. Chen, T. Tsuboi, Appl. Phys. Lett. 92 (2008) 053304.
[20] M.Y. Chan, C.S. Lee, S.L. Lai, M.K. Fung, F.L. Wong, H.Y. Sun, K.M. Lau, S.T. Lee, J. Appl. Phys. 100 (2006) 094506.
[21] P. Peumans, S.R. Forrest, Appl. Phys. Lett. 79 (2001) 126.